

# End-to-End Available Bandwidth: Measurement Methodology, Dynamics, and Relation with TCP Throughput\*

Manish Jain  
Computer and Information Sciences  
University of Delaware  
Newark DE, 19716  
jain@cis.udel.edu

Constantinos Dovrolis<sup>†</sup>  
Computer and Information Sciences  
University of Delaware  
Newark DE, 19716  
dovrolis@cis.udel.edu

## ABSTRACT

The available bandwidth (avail-bw) in a network path is of major importance in congestion control, streaming applications, QoS verification, server selection, and overlay networks. We describe an end-to-end methodology, called Self-Loading Periodic Streams (SLoPS), for measuring avail-bw. The basic idea in SLoPS is that the one-way delays of a periodic packet stream show an increasing trend when the stream's rate is higher than the avail-bw. We implemented SLoPS in a tool called pathload. The accuracy of the tool has been evaluated with both simulations and experiments over real-world Internet paths. Pathload is non-intrusive, meaning that it does not cause significant increases in the network utilization, delays, or losses. We used pathload to evaluate the variability ('dynamics') of the avail-bw in some paths that cross USA and Europe. The avail-bw becomes significantly more variable in heavily utilized paths, as well as in paths with limited capacity (probably due to a lower degree of statistical multiplexing). We finally examine the relation between avail-bw and TCP throughput. A persistent TCP connection can be used to roughly measure the avail-bw in a path, but TCP saturates the path, and increases significantly the path delays and jitter.

## Categories and Subject Descriptors

C.2.3 [Network Operations]: Network Monitoring

---

\*This work was supported by the SciDAC program of the US Department of Energy (award number: DE-FC02-01ER25467).

<sup>†</sup>The authors will join the College of Computing of GATech in August 2002.

Permission to make digital or hard copies of all or part of this work for personal or classroom use is granted without fee provided that copies are not made or distributed for profit or commercial advantage and that copies bear this notice and the full citation on the first page. To copy otherwise, to republish, to post on servers or to redistribute to lists, requires prior specific permission and/or a fee.

SIGCOMM'02, August 19-23, 2002, Pittsburgh, Pennsylvania, USA.  
Copyright 2002 ACM 1-58113-570-X/02/0008 ...\$5.00.

## General Terms

Measurement, Experimentation, Performance

## Keywords

Network capacity, bottleneck bandwidth, bulk transfer capacity, packet pair dispersion, active probing.

## 1. INTRODUCTION

The concept of *available bandwidth*, or *avail-bw* for short, has been of central importance throughout the history of packet networks, in both research and practice. In the context of transport protocols, the robust and efficient use of avail-bw has always been a major issue, including Jacobson's TCP [17]. The avail-bw is also a crucial parameter in capacity provisioning, routing and traffic engineering, QoS management, streaming applications, server selection, and in several other areas.

Researchers have been trying to create end-to-end measurement algorithms for avail-bw over the last 15 years. From Keshav's *packet pair* [22] to Carter and Crovella's *cprobe* [10], the objective was to measure end-to-end avail-bw *accurately*, *quickly*, and without affecting the traffic in the path, i.e., *non-intrusively*. What makes the measurement of avail-bw hard is, first, that there is no consensus on how to precisely define it, second, that it varies with time, and third, that it exhibits high variability in a wide range of timescales.

### 1.1 Definitions

We next define the avail-bw in an intuitive but precise manner. The definition does not depend on higher-level issues, such as the transport protocol or the number of flows that can capture the avail-bw in a path.

A network path  $\mathcal{P}$  is a sequence of  $H$  store-and-forward links that transfer packets from a sender  $SN^D$  to a receiver  $RCV$ . We assume that the path is fixed and unique, i.e., no routing changes or multipath forwarding occur during the measurements. Each link  $i$  can transmit data with a rate  $C_i$  bps, that is referred to as *link capacity*. Two throughput metrics that are commonly associated with  $\mathcal{P}$  are the end-to-end *capacity*  $C$  and *available bandwidth*  $A$ . The capacity is defined as

$$C \equiv \min_{i=1 \dots H} C_i \quad (1)$$

and it is the maximum rate that the path can provide to a flow, when there is no other traffic in  $\mathcal{P}$ .

Suppose that link  $i$  transmitted  $C_i u_i(t_0, t_0 + \tau)$  bits during a time interval  $(t_0, t_0 + \tau)$ . The term  $u_i(t_0, t_0 + \tau)$ , or simply  $u_i^\tau(t_0)$ , is the average utilization of link  $i$  during  $(t_0, t_0 + \tau)$ , with  $0 \leq u_i^\tau(t_0) \leq 1$ . Intuitively, the avail-bw  $A_i^\tau(t_0)$  of link  $i$  in  $(t_0, t_0 + \tau)$  can be defined as the fraction of the link's capacity that has not been utilized during that interval, i.e.,

$$A_i^\tau(t_0) \equiv C_i [1 - u_i^\tau(t_0)] \quad (2)$$

Extending this concept to the entire path, the end-to-end avail-bw  $A^\tau(t_0)$  during  $(t_0, t_0 + \tau)$  is the minimum avail-bw among all links in  $\mathcal{P}$ ,

$$A^\tau(t_0) \equiv \min_{i=1 \dots H} \{C_i [1 - u_i^\tau(t_0)]\} \quad (3)$$

Thus, the end-to-end avail-bw is defined as the maximum rate that the path can provide to a flow, without reducing the rate of the rest of the traffic in  $\mathcal{P}$ .

To avoid the term *bottleneck link*, that has been widely used in the context of both capacity and avail-bw, we introduce two new terms. The *narrow link* is the link with the minimum capacity, and it determines the capacity of the path. The *tight link*, on the other hand, is the link with the minimum avail-bw, and it determines the avail-bw of the path.

The parameter  $\tau$  in (3) is the avail-bw *averaging timescale*. If we consider  $A^\tau(t)$  as a stationary random process, the variance  $\text{Var}\{A^\tau\}$  of the process decreases as the averaging timescale  $\tau$  increases. We note that if  $A^\tau$  is self-similar, the variance  $\text{Var}\{A^\tau\}$  decreases slowly, in the sense that the decrease of  $\text{Var}\{A^\tau\}$  as  $\tau$  increases is slower than the reciprocal of  $\tau$  [26].

## 1.2 Main contributions

In this paper, we present an original end-to-end avail-bw measurement methodology, called *Self-Loading Periodic Streams* or *SLoPS*. The basic idea in SLoPS is that the one-way delays of a periodic packet stream show an increasing trend when the stream's rate is higher than the avail-bw. SLoPS has been implemented in a measurement tool called *pathload*. The tool has been verified experimentally, by comparing its results with MRTG utilization graphs for the path links [33]. We have also evaluated *pathload* in a controlled and reproducible environment using NS simulations. The simulations show that *pathload* reports a range that includes the average avail-bw in a wide range of load conditions and path configurations. The tool underestimates the avail-bw, however, when the path includes several tight links. The *pathload* measurements are non-intrusive, meaning that they do not cause significant increases in the network utilization, delays, or losses. *Pathload* is described in detail in a different publication [19]; here we describe the tool's salient features and show a few experimental and simulation results to evaluate the tool's accuracy.

An important feature of *pathload* is that, instead of reporting a single figure for the average avail-bw in a time interval  $(t_0, t_0 + \Theta)$ , it estimates the range in which the avail-bw process  $A^\tau(t)$  varies in  $(t_0, t_0 + \Theta)$ , when it is measured with an averaging timescale  $\tau < \Theta$ . The timescales  $\tau$  and  $\Theta$  are related to two tool parameters, namely the 'stream duration' and the 'fleet duration'.

We have used *pathload* to estimate the variability (or 'dynamics') of the avail-bw in different paths and load condi-

tions. An important observation is that the avail-bw becomes more variable as the utilization of the tight link increases (i.e., as the avail-bw decreases). Similar observations are made for paths of different capacity that operate at about the same utilization. Specifically, the avail-bw shows higher variability in paths with smaller capacity, probably due to a lower degree of statistical multiplexing.

Finally, we examined the relation between the avail-bw and the throughput of a 'greedy' TCP connection, i.e., a persistent bulk transfer with sufficiently large advertised window. Our experiments show that such a greedy TCP connection can be used to roughly measure the end-to-end avail-bw, but TCP saturates the path, increases significantly the delays and jitter, and potentially causes losses to other TCP flows. The increased delays and losses in the path cause other TCP flows to slow down, allowing the greedy TCP connection to grab more bandwidth than what was previously available.

## 1.3 Overview

§2 summarizes previous work on bandwidth estimation. §3 explains the SLoPS measurement methodology. §4 describes the *pathload* implementation. §5 presents simulation and experimental verification results. §6 evaluates the dynamics of avail-bw using *pathload*. §7 examines the relation between avail-bw and TCP throughput. §8 shows that *pathload* is not network intrusive. The paper concludes with a number of applications in §9.

## 2. RELATED WORK

Although there are several bandwidth estimation tools, most of them measure capacity rather than avail-bw. Specifically, *pathchar* [18], *clink* [13], *pchar* [27], and the *tailgating* technique of [24] measure *per-hop capacity*. Also, *bprobe* [10], *nettimer* [23], *pathrate* [12], and the *PBM* methodology [36] measure *end-to-end capacity*.

Allman and Paxson noted that an avail-bw estimate can give a more appropriate value for the *ssthresh* variable, improving the slow-start phase of TCP [2]. They recognized, however, the complexity of measuring avail-bw from the timing of TCP packets, and they focused instead on capacity estimates.

The first tool that attempted to measure avail-bw was *cprobe* [10]. *cprobe* estimated the avail-bw based on the dispersion of long packet trains at the receiver. A similar approach was taken in *pipechar* [21]. The underlying assumption in these works is that the dispersion of long packet trains is inversely proportional to the avail-bw. Recently, however, [12] showed that this is not the case. The dispersion of long packet trains does not measure the avail-bw in a path; instead, it measures a different throughput metric that is referred to as *Asymptotic Dispersion Rate* (ADR).

A different avail-bw measurement technique, called *Delphi*, was proposed in [37]. The main idea in Delphi is that the spacing of two probing packets at the receiver can provide an estimate of the amount of traffic at a link, provided that the queue of that link does not empty between the arrival times of the two packets. *Delphi* assumes that the path can be well modeled by a single queue. This model is not applicable when the tight and narrow links are different, and it interprets queueing delays anywhere in the path as queueing delays at the tight link.

Another technique, called *TOPP*, for measuring avail-bw

was proposed in [30]. TOPP uses sequences of packet pairs sent to the path at increasing rates. From the relation between the input and output rates of different packet pairs, one can estimate the avail-bw and the capacity of the tight link in the path. In certain path configurations, it is possible to also measure the avail-bw and capacity of other links in the path<sup>1</sup>. Both TOPP and our technique, SLoPS, are based on the observation that the queueing delays of successive periodic probing packets increase when the probing rate is higher than the avail-bw in the path. The two techniques, however, are quite different in the actual algorithm they use to estimate the avail-bw. A detailed comparison of the two estimation methods is an important task for further research.

A different definition of ‘available capacity’ was given in [6]. The *available capacity* is defined as the amount of data that can be inserted into a network path at a certain time, so that the transit delay of these packets would be bounded by a given maximum permissible delay.

Paxson defined and measured a *relative avail-bw metric*  $\beta$  [36]. His metric is based on the one-way delay variations of a flow’s packets.  $\beta$  measures the proportion of packet delays that are due to the flow’s own load. If each packet was only queued behind its predecessors, the path is considered empty and  $\beta \approx 1$ . On the other hand, if the observed delay variations are mostly due to cross traffic, the path is considered saturated and  $\beta \approx 0$ . Unfortunately, there is no direct relationship between  $\beta$  and the avail-bw in the path or the utilization of the tight link.

An issue of major importance is the *predictability* of the avail-bw. Paxson’s metric  $\beta$  is fairly predictable: on average, a measurement of  $\beta$  at a given path falls within 10% of later  $\beta$  measurements for periods that last for several hours [36]. Balakrishnan et.al. examined the throughput stationarity of successive Web transfers to a set of clients [5]. The throughput to a given client appeared to be *piecewise stationary* in timescales that extend for hundreds of minutes. Additionally, the throughput of successive transfers to a given client varied by less than a factor of 2 over three hours. A more elaborate investigation of the stationarity of avail-bw was recently published in [39]. Zhang et.al. measured the TCP throughput of 1MB transfers every minute for five hours. Their dataset includes 49,000 connections in 145 distinct paths. They found out that the throughput *Change Free Regions*, i.e., the time periods in which the throughput time series can be modeled as a stationary process, often last for more than an hour. Also, the throughput stays in a range with peak-to-peak variation of a factor of 3 for several hours. An important point is that these previous works did not correlate the variability of avail-bw with the operating conditions in the underlying paths. We attempt such an approach in §6.

To characterize the ability of a path to transfer large files using TCP, the IETF recommends the *Bulk-Transfer-Capacity (BTC)* metric [29]. The BTC of a path in a certain time period is the throughput of a persistent (or ‘bulk’) TCP transfer through that path, when the transfer is only limited by the network resources and not by buffer, or other, limitations at the end-systems. The BTC can be measured

with *Treno* [28] or *cap* [1]. It is important to distinguish between the avail-bw and the BTC of a path. The former gives the total spare capacity in the path, independent of which transport protocol attempts to capture it. The latter, on the other hand, depends on TCP’s congestion control, and it is the maximum throughput that a *single and persistent* TCP connection can get. Parallel persistent connections, or a large number of short TCP connections (‘mice’), can obtain an aggregate throughput that is higher than the BTC. The relation between BTC and avail-bw is investigated in §7.

Finally, several congestion control algorithms, such as those proposed in [31, 20, 8, 4], infer that the path is congested (or that there is no avail-bw) when the round-trip delays in the path start increasing. This is similar to the basic idea of our estimation methodology: the one-way delays of a periodic packet stream are expected to show an increasing trend when the stream’s rate is higher than the avail-bw. The major difference between SLoPS and those proposals is that we use the relation between the probing rate and the observed delay variations to develop an elaborate avail-bw measurement algorithm, rather than a congestion control algorithm. Also, SLoPS is based on periodic rate-controlled streams, rather than window-controlled transmissions, allowing us to compare a certain rate with the avail-bw more reliably.

### 3. SELF-LOADING PERIODIC STREAMS

In this section, we describe the Self-Loading Periodic Streams (*SLoPS*) measurement methodology. A periodic stream in SLoPS consists of  $K$  packets of size  $L$ , sent to the path at a constant rate  $R$ . If the stream rate  $R$  is higher than the avail-bw  $A$ , the one-way delays of successive packets at the receiver show an increasing trend. We first illustrate this fundamental effect in its simplest form through an analytical model with stationary and fluid cross traffic. Then, we show how to use this ‘increasing delays’ property in an iterative algorithm that measures end-to-end avail-bw. Finally, we depart from the previous fluid model, and observe that the avail-bw may vary during a stream. This requires us to refine SLoPS in several ways, that is the subject of the next section.

#### 3.1 SLoPS with fluid cross traffic

Consider a path from  $\mathcal{SND}$  to  $\mathcal{RCV}$  that consists of  $H$  links,  $i = 1, \dots, H$ . The capacity of link  $i$  is  $C_i$ . We consider a stationary (i.e., time invariant) and fluid model for the cross traffic in the path. So, if the avail-bw at link  $i$  is  $A_i$ , the utilization is  $u_i = (C_i - A_i)/C_i$  and there are  $u_i C_i \tau$  bytes of cross traffic departing from, and arriving at, link  $i$  in any interval of length  $\tau$ . Also, assume that the links follow the First-Come First-Served queueing discipline<sup>2</sup>, and that they are adequately buffered to avoid losses. We ignore any propagation or fixed delays in the path, as they do not affect the delay variation between packets. The avail-bw  $A$  in the path is determined by the tight link  $t \in \{1, \dots, H\}$  with<sup>3</sup>

$$A_t = \min_{i=1 \dots H} A_i = \min_{i=1 \dots H} C_i (1 - u_i) = A \quad (4)$$

<sup>2</sup>In links with per-flow or per-class queueing, SLoPS can obviously monitor the sequence of queues that the probing packets go through.

<sup>3</sup>If there are more than one links with avail-bw  $A$ , the tight link is the first of them, without loss of generality.

<sup>1</sup>In [19], we incorrectly stated that TOPP’s accuracy depends on the order of the links in the path. Even though this is true for an arbitrary link in the path, TOPP is able to estimate the avail-bw and capacity of the tight link.

Suppose that  $\mathcal{SND}$  sends a periodic stream of  $K$  packets to  $\mathcal{RCV}$  at a rate  $R_0$ , starting at an arbitrary time instant. The packet size is  $L$  bytes, and so packets are sent with a period of  $T = L/R_0$  time units. The One-Way Delay (OWD)  $D^k$  from  $\mathcal{SND}$  to  $\mathcal{RCV}$  of packet  $k$  is

$$D^k = \sum_{i=1}^H \left( \frac{L}{C_i} + \frac{q_i^k}{C_i} \right) = \sum_{i=1}^H \left( \frac{L}{C_i} + d_i^k \right) \quad (5)$$

where  $q_i^k$  is the queue size at link  $i$  upon the arrival of packet  $k$  ( $q_i^k$  does not include packet  $k$ ), and  $d_i^k = q_i^k/C_i$  is the queueing delay of packet  $k$  at link  $i$ . The OWD difference between two successive packets  $k$  and  $k+1$  is

$$\Delta D^k \equiv D^{k+1} - D^k = \sum_{i=1}^H \frac{\Delta q_i^k}{C_i} = \sum_{i=1}^H \Delta d_i^k \quad (6)$$

where  $\Delta q_i^k \equiv q_i^{k+1} - q_i^k$ , and  $\Delta d_i^k \equiv \Delta q_i^k/C_i$ .

We can now show that, if  $R_0 > A$  the  $K$  packets of the periodic stream will arrive at  $\mathcal{RCV}$  with increasing OWDs, while if  $R_0 \leq A$  the stream packets will encounter equal OWDs. This property is stated next, and proved in Appendix A.

**PROPOSITION 1.** *If  $R_0 > A$ , then  $\Delta D^k > 0$  for  $k = 1, \dots, K-1$ . Else, if  $R_0 \leq A$ ,  $\Delta D^k = 0$  for  $k = 1, \dots, K-1$ .*

One may think that the avail-bw  $A$  can be computed directly from the rate at which the stream arrives at  $\mathcal{RCV}$ . This is the approach followed in packet train dispersion techniques. The following result, however, shows that, in a general path configuration, this would be possible only if the capacity and avail-bw of all links (except the avail-bw of the tight link) are *a priori* known.

**PROPOSITION 2.** *The rate  $R_H$  of the packet stream at  $\mathcal{RCV}$  is a function, in the general case, of  $C_i$  and  $A_i$  for all  $i = 1, \dots, H$ .*

This result follows from the proof in Appendix A (apply recursively Equation 19 until  $i = H$ ).

### 3.2 An iterative algorithm to measure $A$

Based on Proposition 1, we can construct an iterative algorithm for the end-to-end measurement of  $A$ . Suppose that  $\mathcal{SND}$  sends a periodic stream  $n$  with rate  $R(n)$ . The receiver analyzes the OWD variations of the stream, based on Proposition 1, to determine whether  $R(n) > A$  or not. Then,  $\mathcal{RCV}$  notifies  $\mathcal{SND}$  about the relation between  $R(n)$  and  $A$ . If  $R(n) > A$ ,  $\mathcal{SND}$  sends the next periodic stream  $n+1$  with rate  $R(n+1) < R(n)$ . Otherwise, the rate of stream  $n+1$  is  $R(n+1) > R(n)$ .

Specifically,  $R(n+1)$  can be computed as follows,

$$\begin{aligned} \text{If } R(n) > A, R^{max} &= R(n); \\ \text{If } R(n) \leq A, R^{min} &= R(n); \\ R(n+1) &= (R^{max} + R^{min})/2; \end{aligned} \quad (7)$$

$R^{min}$  and  $R^{max}$  are lower and upper bounds for the avail-bw after stream  $n$ , respectively. Initially,  $R^{min}=0$  and  $R^{max}$  can be set to a sufficiently high value  $R_0^{max} > A$ .<sup>4</sup> The algorithm terminates when  $R^{max} - R^{min} \leq \omega$ , where  $\omega$  is the user-specified *estimation resolution*. If the avail-bw  $A$  does

<sup>4</sup>A better way to initialize  $R^{max}$  is described in [19].

not vary with time, the previous algorithm will converge to a range  $[R^{min}, R^{max}]$  that includes  $A$  after  $\lceil \log_2(R_0^{max}/\omega) \rceil$  streams.

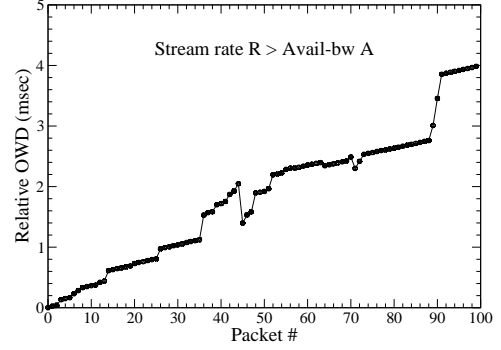


**Figure 1:** OWD variations for a periodic stream when  $R > A$ .

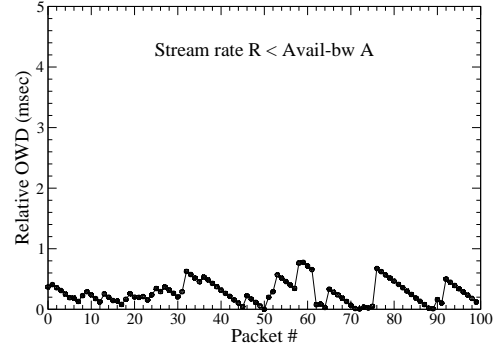


**Figure 2:** OWD variations for a periodic stream when  $R < A$ .

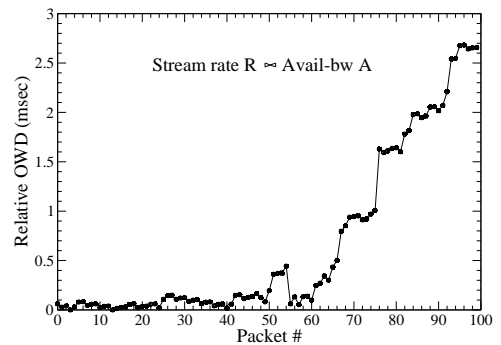


**Figure 3:** OWD variations for a periodic stream when  $R \approx A$ .

### 3.3 SLoPS with real cross traffic

We assumed so far that the avail-bw  $A$  is constant during the measurement process. In reality, the avail-bw may vary because of two reasons. First, the avail-bw process  $A^T(t)$  of (3) may be non-stationary, and so its expected value may

also be a function of time. Even if  $A^\tau(t)$  is stationary, however, the process  $A^\tau$  can have a significant statistical variability around its (constant) mean  $E[A^\tau]$ , and to make things worse, this variability may extend over a wide range of timescales  $\tau$ . How can we refine SLoPS to deal with the dynamic nature of the avail-bw process?

To gain some insight into this issue, Figures 1, 2, and 3 show the OWD variations in three periodic streams that crossed a 12-hop path from Univ-Oregon to Univ-Delaware. All three streams have  $K=100$  packets with  $T=100\mu s$ . The 5-minute average avail-bw in the path during these measurements was about 74Mbps, according to the MRTG utilization graph of the tight link (see Appendix B). In Figure 1, the stream rate is  $R=96$ Mbps, i.e., higher than the long-term avail-bw. Notice that the OWDs between successive packets are not strictly increasing, as one would expect from Proposition 1, but *overall, the stream OWDs have a clearly increasing trend*. This is shown both by the fact that most packets have a higher OWD than their predecessors, and because the OWD of the last packet is about 4ms larger than the OWD of the first packet. On the other hand, the stream of Figure 2 has a rate  $R=37$ Mbps, i.e., lower than the long-term avail-bw. Even though there are short-term intervals in which we observe increasing OWDs, *there is clearly not an increasing trend in the stream*. The third stream, in Figure 3, has a rate  $R=82$ Mbps. The stream does not show an increasing trend in the first half, indicating that the avail-bw during that interval is higher than  $R$ . The situation changes dramatically, however, after roughly the 60-th packet. In that second half of the stream there is a clear increasing trend, showing that the avail-bw decreases to less than  $R$ .

The previous example motivates two important refinements in the SLoPS methodology. First, instead of analyzing the OWD variations of a stream, expecting one of the two cases of Proposition 1 to be strictly true for every pair of packets, we should instead watch for the presence of *an overall increasing trend during the entire stream*. Second, we have to accept the possibility that the avail-bw may vary around rate  $R$  during a probing stream. In that case, there is no strict ordering between  $R$  and  $A$ , and thus a third possibility comes up, that we refer to as ‘grey-region’ (denoted as  $R \bowtie A$ ). The next section gives a concrete specification of these two refinements, as implemented in *pathload*.

## 4. MEASUREMENT TOOL: *PATHLOAD*

We implemented SLoPS in a tool called *pathload*<sup>5</sup>. *Pathload*, together with its experimental verification, is described in detail in [19]. In this section, we provide a description of the tool’s salient features.

*Pathload* consists of a process  $\mathcal{SND}$  running at the sender, and a process  $\mathcal{RCV}$  running at the receiver. The stream packets use UDP, while a TCP connection between the two end-points controls the measurements.

### 4.1 Clock and timing issues

$\mathcal{SND}$  timestamps each packet upon its transmission. So,  $\mathcal{RCV}$  can measure the *relative OWD*  $D^k$  of packet  $k$ , that differs from the actual OWD by a certain offset. This offset is due to the non-synchronized clocks of the end-hosts.

<sup>5</sup>The source code for both *pathrate* and *pathload* is available at <http://www.pathrate.org>.

Since we are only interested in OWD differences though, a constant offset in the measured OWDs does not affect the analysis. Clock skew can be a potential problem,<sup>6</sup> but not in *pathload*. The reason is that each stream lasts for only a few milliseconds (§4.2), and so the skew during a stream is in the order of nanoseconds, much less than the OWD variations due to queueing. Also, *pathload* uses techniques (described in [19]) to detect context-switches at the end-hosts.

### 4.2 Stream parameters

A stream consists of  $K$  packets of size  $L$ , sent at a constant rate  $R$ .  $R$  is adjusted at run-time for each stream, as described in §4.6. The packet inter-spacing  $T$  is normally set to  $T_{min}$ , and is achieved with ‘busy-waiting’ at the sending process.  $T_{min}$  is currently set to  $100\mu sec$ ; in the next release of the tool, however, this value will be automatically configured based on the minimum possible period that the end-hosts can achieve. The receiver measures the inter-spacing  $T$  with which the packets left the sender, using the  $\mathcal{SND}$  timestamps, to detect context switches and other rate deviations [19].

Given  $R$  and  $T$ , the packet size is computed as  $L = RT$ .  $L$ , however, has to be smaller than the path MTU  $L^{max}$  (to avoid fragmentation), and larger than a minimum possible size  $L^{min}=200B$ . The reason for the  $L^{min}$  constraint is to reduce the effect of Layer-2 headers on the stream rate (see [34]). If  $R < L^{min}/T_{min}$ , the inter-spacing  $T$  is increased to  $L^{min}/R$ . The maximum rate that *pathload* can generate, and thus the maximum avail-bw that it can measure, is  $L^{max}/T_{min}$ . In the current release (with  $T_{min}=100\mu sec$ ), the maximum rate is 120Mbps for an Ethernet MTU, which is sufficiently high to measure a Fast-Ethernet limited path.

The stream length  $K$  is chosen based on two constraints. First, a stream should be relatively short, so that it does not cause large queues and potentially losses in the path routers. Second,  $K$  controls the *stream duration*  $V = KT$ , which is related to the *averaging timescale*  $\tau$  (see §6.3). A larger  $K$  (longer stream) increases  $\tau$ , and thus reduces the variability in the measured avail-bw. In *pathload*, the default value for  $K$  is 100 packets. Thus, with  $L=800B$  and  $T=100\mu sec$ , a stream carries 80,000 bytes and it lasts for 10msec.

### 4.3 Detecting an increasing OWD trend

Suppose that the (relative) OWDs of a particular stream are  $D^1, D^2, \dots, D^K$ . As a pre-processing step, we partition these measurements into  $\Gamma = \sqrt{K}$  groups of  $\Gamma$  consecutive OWDs. Then, we compute the median OWD  $\hat{D}^k$  of each group. *Pathload* analyzes the set  $\{\hat{D}^k, k = 1, \dots, \Gamma\}$ , which is more robust to outliers and errors.

We use two complementary statistics to check if a stream shows an increasing trend. The *Pairwise Comparison Test* (PCT) metric of a stream is

$$S_{PCT} = \frac{\sum_{k=2}^{\Gamma} I(\hat{D}^k > \hat{D}^{k-1})}{\Gamma - 1} \quad (8)$$

where  $I(X)$  is one if  $X$  holds, and zero otherwise. PCT measures the fraction of consecutive OWD pairs that are increasing, and so  $0 \leq S_{PCT} \leq 1$ . If the OWDs are independent, the expected value of  $S_{PCT}$  is 0.5. If there is a strong increasing trend,  $S_{PCT}$  approaches one.

<sup>6</sup>And there are algorithms to remove its effects [35].

The *Pairwise Difference Test* (PDT) metric of a stream is

$$S_{PDT} = \frac{\hat{D}^\Gamma - \hat{D}^1}{\sum_{k=2}^\Gamma |\hat{D}^k - \hat{D}^{k-1}|} \quad (9)$$

PDT quantifies how strong is the start-to-end OWD variation, relative to the OWD absolute variations during the stream. Note that  $-1 \leq S_{PDT} \leq 1$ . If the OWDs are independent, the expected value of  $S_{PDT}$  is zero. If there is a strong increasing trend,  $S_{PDT}$  approaches one.

In the current release of *pathload*, the PCT metric shows an increasing trend if  $S_{PCT} > 0.55$ , while the PDT shows increasing trend if  $S_{PDT} > 0.4$ . These two threshold values for  $S_{PCT}$  and  $S_{PDT}$  (0.55 and 0.4, respectively) were chosen after extensive simulations of *pathload* in paths with varying load conditions, path configurations, and traffic models.

There are cases in which one of the two metrics is better than the other in detecting an increasing trend (see [19]). Consequently, if either the PCT or PDT metrics shows an ‘increasing trend’, *pathload* characterizes the stream as *type-I*, i.e., increasing. Otherwise, the stream is considered of *type-N*, i.e., non-increasing.

#### 4.4 Fleets of streams

*Pathload* does *not* determine whether  $R > A$  based on a single stream. Instead, it sends a *fleet* of  $N$  streams, so that it samples whether  $R > A$   $N$  successive times. All streams in a fleet have the same rate  $R$ . Each stream is sent only when the previous stream has been acknowledged, to avoid a backlog of streams in the path. So, there is always an idle interval  $\Delta$  between streams, which is larger than the Round-Trip Time (RTT) of the path. The duration of a fleet is  $U = N(V + \Delta) = N(KT + \Delta)$ . Given  $V$  and  $\Delta$ ,  $N$  determines the fleet duration, which is related to the *pathload* measurement latency. The default value for  $N$  is 12 streams. The effect of  $N$  is discussed in §6.4.

The average *pathload* rate during a fleet of rate  $R$  is

$$\frac{NKL}{N(V + \Delta)} = R \frac{1}{1 + \frac{\Delta}{V}}$$

In order to limit the average *pathload* rate to less than 10% of  $R$ , the current version<sup>7</sup> of *pathload* sets the inter-stream latency to  $\Delta = \max\{RTT, 9V\}$ .

If a stream encounters excessive losses (>10%), or if more than a number of streams within a fleet encounter moderate losses (>3%), the entire fleet is aborted and the rate of the next fleet is decreased. For more details, see [19].

#### 4.5 Grey-region

If a large fraction  $f$  of the  $N$  streams in a fleet are of type-I, the entire fleet shows an increasing trend and we infer that the fleet rate is larger than the avail-bw ( $R > A$ ). Similarly, if a fraction  $f$  of the  $N$  streams are of type-N, the fleet does not show an increasing trend and we infer that the fleet rate is smaller than the avail-bw ( $R < A$ ). It can happen, though, that less than  $N \times f$  streams are of type-I, and also that less than  $N \times f$  streams are of type-N. In that case, some streams ‘sampled’ the path when the avail-bw was less than  $R$  (type-I), and some others when it was more than  $R$  (type-N). We say, then, that the fleet rate  $R$  is in the ‘grey-region’ of the avail-bw, and write  $R \bowtie A$ . The interpretation that we give to the grey-region is that *when  $R \bowtie A$ , the avail-bw*

*process  $A^\tau(t)$  during that fleet varied above and below rate  $R$ , causing some streams to be of type-I and some others to be of type-N*. The averaging timescale  $\tau$ , here, is related to the stream duration  $V$ .

In the current release of *pathload*,  $f$  is set to 70%. A higher  $f$  can increase the width of the estimated avail-bw range, because of a larger grey-region. On the other hand, a lower  $f$  (but higher than 50%) can mislead the tool that  $R > A$  or  $R < A$ , even though  $R \bowtie A$ , producing an incorrect final estimate. A sensitivity analysis for  $f$ , as well as for the PCT and PDT thresholds, is a task that we are currently working on.

#### 4.6 Rate adjustment algorithm

After a fleet  $n$  of rate  $R(n)$  is over, *pathload* determines whether  $R(n) > A$ ,  $R(n) < A$ , or  $R(n) \bowtie A$ . The iterative algorithm that determines the rate  $R(n+1)$  of the next fleet is quite similar to the binary-search approach of (7). There are two important differences though.

First, together with the upper and lower bounds for the avail-bw  $R^{max}$  and  $R^{min}$ , *pathload* also maintains upper and lower bounds for the grey-region, namely  $G^{max}$  and  $G^{min}$ . When  $R(n) \bowtie A$ , one of these bounds is updated depending on whether  $G^{max} < R(n) < R^{max}$  (update  $G^{max}$ ), or  $G^{min} > R(n) > R^{min}$  (update  $G^{min}$ ). If a grey-region has not been detected up to that point, the next rate  $R(n+1)$  is chosen, as in (7), half-way between  $R^{min}$  and  $R^{max}$ . If a grey-region has been detected,  $R(n+1)$  is set half-way between  $G^{max}$  and  $R^{max}$  when  $R(n) = G^{max}$ , or half-way between  $G^{min}$  and  $R^{min}$  when  $R(n) = G^{min}$ . The complete rate adjustment algorithm, including the initialization steps, is given in [19]. It is important to note that this binary-search approach succeeds in converging to the avail-bw, as long as the avail-bw variation range is strictly included in the  $[R^{min}, R^{max}]$  range. The experimental and simulation results of the next section show that this is the case generally, with the exception of paths that include several tight links.

The second difference is that *pathload* terminates not only when the avail-bw has been estimated within a certain resolution  $\omega$  (i.e.,  $R^{max} - R^{min} \leq \omega$ ), but also when  $R^{max} - G^{max} \leq \chi$  and  $G^{min} - R^{min} \leq \chi$ , i.e., when both avail-bw boundaries are within  $\chi$  from the corresponding grey-region boundaries. The parameter  $\chi$  is referred to as *grey-region resolution*.

The tool eventually reports the range  $[R^{min}, R^{max}]$ .

#### 4.7 Measurement latency

Since *pathload* is based on an iterative algorithm, it is hard to predict how long will a measurement take. For the default tool parameters, and for a path with  $A \approx 100$ Mbps and  $\Delta = 100$ ms, the tool needs less than 15 seconds to produce a final estimate. The measurement latency increases as the absolute magnitude of the avail-bw and/or the width of the grey-region increase, and it also depends on the resolution parameters  $\omega$  and  $\chi$ .

<sup>7</sup>As of June 2002, the current version of *pathload* is 1.0.2

## 5. VERIFICATION

The objective of this section is to evaluate the accuracy of *pathload* with both NS simulations [32], and experiments over real Internet paths.

### 5.1 Simulation results

The following simulations evaluate the accuracy of *pathload* in a controlled and reproducible environment under various load conditions and path configurations. Specifically, we implemented the *pathload* sender (*SN*) and receiver (*RCV*) in application-layer NS modules. The functionality of these modules is identical as in the original *pathload*, with the exception of some features that are not required in a simulator (such as the detection of context switches).

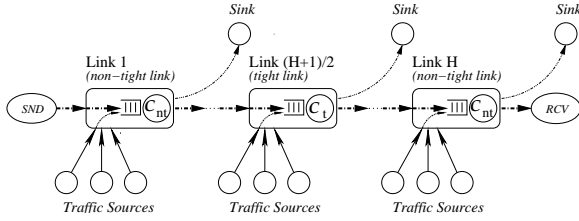


Figure 4: Simulation topology.

In the following, we simulate the  $H$ -hop topology of Figure 4. The *pathload* packets enter the path in hop 1 and exit at hop  $H$ . The hop in the middle of the path is the tight link, and it has capacity  $C_t$ , avail-bw  $A_t$ , and utilization  $u_t$ . We refer to the rest of the links as *non-tight*, and consider the case where they all have the same capacity  $C_{nt}$ , avail-bw  $A_{nt}$ , and utilization  $u_{nt}$ . Cross-traffic is generated at each link from ten random sources that, unless specified otherwise, generate Pareto interarrivals with  $\alpha=1.9$ . The cross-traffic packet sizes are distributed as follows: 40% are 40B, 50% are 550B, and 10% are 1500B. The end-to-end propagation delay in the path is 50 msec, and the links are sufficiently buffered to avoid packet losses.

We next examine the effect of cross-traffic load in the tight and non-tight links on the accuracy of *pathload*, i.e., the effect of  $u_t$  and  $u_{nt}$ , as well as the effect of the number of hops  $H$ . Another important factor is the relative magnitude of the avail-bw in the non-tight links  $A_{nt}$  and in the tight link  $A_t$ . To quantify this, we define the *path tightness factor* as

$$\beta = \frac{A_{nt}}{A_t} \geq 1 \quad (10)$$

Unless specified otherwise, the default parameters in the following simulations are  $H=5$  hops,  $C_t=10$ Mbps,  $\beta=5$ , and  $u_t=u_{nt}=60\%$ .

Figure 5 examines the accuracy of *pathload* in four tight link utilization values, ranging from light load ( $u_t=30\%$ ) to heavy load ( $u_t=90\%$ ). We also consider two cross-traffic models: exponential interarrivals and Pareto interarrivals with infinite variance ( $\alpha=1.5$ ). For each utilization and traffic model, we run *pathload* 50 times to measure the avail-bw in the path. After each run, the tool reports a range  $[R^{min}, R^{max}]$  in which the avail-bw varies. The *pathload* range that we show in Figure 5 results from averaging the 50 lower bounds  $R^{min}$  and the 50 upper bounds  $R^{max}$ . The coefficient of variation for the 50 samples of  $R^{min}$  and  $R^{max}$

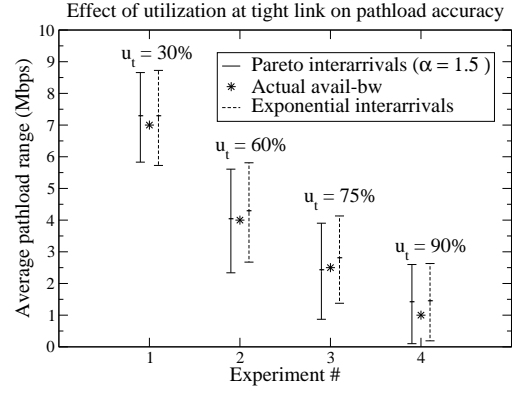


Figure 5: Simulation results for different traffic types and tight link loads.

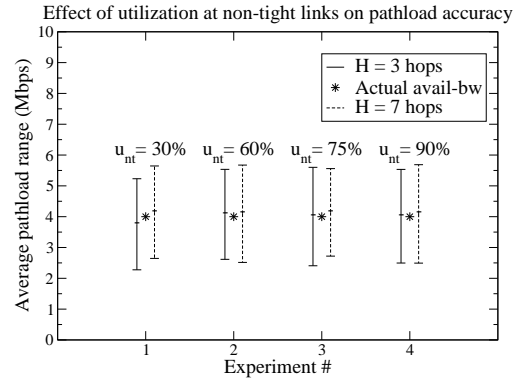


Figure 6: Simulation results for different non-tight link loads.

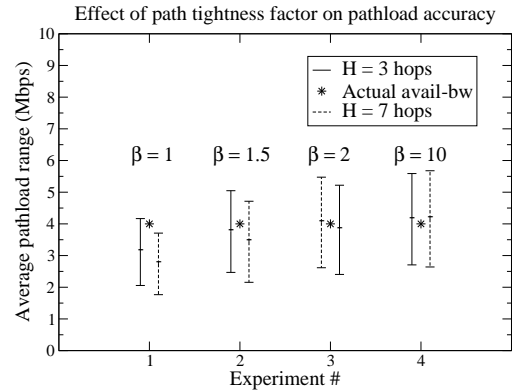


Figure 7: Simulation results for different path tightness factors  $\beta$ .

in the following simulations was typically between 0.10 and 0.30.

The main observation in Figure 5 is that *pathload* produces a range that includes the average avail-bw in the path, in both light and heavy load conditions at the tight link. This is true with both the smooth interarrivals of Poisson traffic, and with the infinite-variance Pareto model. For instance,

when the avail-bw is 4Mbps, the average *pathload* range in the case of Pareto interarrivals is from 2.4 to 5.6 Mbps. It is also important to note that the center of the *pathload* range is relatively close to the average avail-bw. In Figure 5, the maximum deviation between the average avail-bw and the center of the *pathload* range is when the former is 1Mbps and the latter is 1.5Mbps.

The next issue is whether the accuracy of *pathload* depends on the number and load of the non-tight links. Figure 6 shows, as in the previous paragraph, 50-sample average *pathload* ranges for four different utilization points  $u_{nt}$  at the non-tight links, and for two different path lengths  $H$ . Since  $C_t=10\text{Mbps}$  and  $u_t=60\%$ , the end-to-end avail-bw in these simulations is 4Mbps. The path tightness factor is  $\beta=5$ , and so the avail-bw in the non-tight links is  $A_{nt}=20\text{Mbps}$ . So, even when there is significant load and queueing at the non-tight links (which is the case when  $u_{nt}=90\%$ ), the end-to-end avail-bw is quite lower than the avail-bw in the  $H-1$  non-tight links.

The main observation in Figure 6 is that *pathload* estimates a range that includes the actual avail-bw in all cases, independent of the number of non-tight links or of their load. Also, the center of the *pathload* range is within 10% of the average avail-bw  $A_t$ . So, when the end-to-end avail-bw is mostly limited by a single link, *pathload* is able to estimate accurately the avail-bw in a multi-hop path even when there are several other queueing points. The non-tight links introduce noise in the OWDs of *pathload* streams, but they do not affect the OWD trend that is formed when the stream goes through the tight link.

Finally, we examine whether the accuracy of *pathload* depends on the path tightness factor  $\beta$ . Figure 7 shows 50-sample average *pathload* ranges for four different values of  $\beta$ , and for two different path lengths  $H$ . As previously,  $C_t=10\text{Mbps}$ ,  $u_t=60\%$ , and so the average avail-bw is  $A_t=4\text{Mbps}$ . Note that when the path tightness factor is  $\beta=1$ , all  $H$  links have the same avail-bw  $A_{nt}=A_t=4\text{Mbps}$ , meaning that they are all tight links. The main observation in Figure 7 is that *pathload* succeeds in estimating a range that includes the actual avail-bw when there is only one tight link in the path, but it underestimates the avail-bw when there are multiple tight links.

To understand the nature of this problem, note that an underestimation occurs when  $R^{max}$  is set to a fleet rate  $R$ , even though  $R$  is less than the avail-bw  $A_t$ . Recall that *pathload* sets the state variable  $R^{max}$  to a rate  $R$  when more than  $f=70\%$  of a fleet's streams have an increasing delay trend. A stream of rate  $R$ , however, can get an increasing delay trend at any link of the path in which the avail-bw during the stream is less than  $R$ . Additionally, after a stream gets an increasing delay trend it is unlikely that it will loose that trend later in the path. Consider a path with  $H_t$  tight links, all of them having an average avail-bw  $A_t$ . Suppose that  $p$  is the probability that a stream of rate  $R$  will get an increasing delay trend at a tight link, even though  $R < A_t$ . Assuming that the avail-bw variations at different links are independent, the probability that the stream will have an increasing delay trend after  $H_t$  tight links is  $1 - (1-p)^{H_t}$ , that increases very quickly with  $H_t$ . This explains why the underestimation error in Figure 7 appears when  $\beta$  is close to one (i.e.,  $H_t > 1$ ), and why it is more significant with  $H_t=7$  rather than with 3 hops.

## 5.2 Experimental results

We have also verified *pathload* experimentally, comparing its output with the avail-bw shown in the MRTG graph of the path's tight link. More information about how we used MRTG in these experiments is given in Appendix B. Even though this verification methodology is not too accurate, it was the only way in which we could evaluate *pathload* in real and wide-area Internet paths.

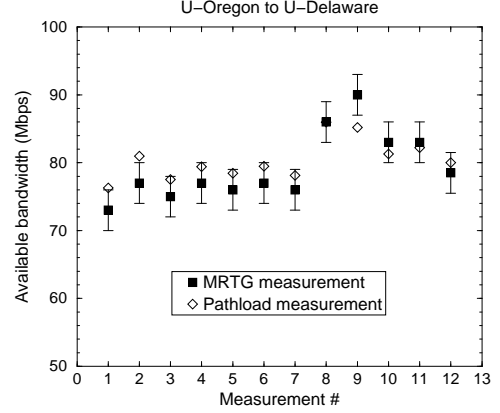


Figure 8: Verification experiment #1.

In the experiments of Figures 8 and 9, the resolution parameters were  $\omega=1\text{Mbps}$  and  $\chi=1.5\text{Mbps}$ . We also note that these results were generated from an older version of *pathload* in which the PCT and PDT thresholds were 0.6 and 0.5 (instead of 0.55 and 0.4), respectively.

An MRTG reading is a 5-minute average avail-bw. *Pathload*, however, takes about 10-30 seconds to produce an estimate. To compare these short-term *pathload* estimates with the MRTG average, we run *pathload* consecutively for 5 minutes. Suppose that in a 5-min (300sec) interval we run *pathload*  $W$  times, and that run  $i$  lasted for  $q_i$  seconds, reporting an avail-bw range  $[R_i^{min}, R_i^{max}]$  ( $i = 1, \dots, W$ ). The 5-min average avail-bw  $\hat{R}$  that we report here for *pathload* is the following weighted average of  $(R_i^{min} + R_i^{max})/2$ :

$$\hat{R} = \sum_{i=1}^W \frac{q_i}{300} \frac{R_i^{min} + R_i^{max}}{2} \quad (11)$$

Figure 8 shows the MRTG and *pathload* results for 12 independent runs in a path from a Univ-Oregon host to a Univ-Delaware host.<sup>8</sup> An interesting point about this path is that the tight link is different than the narrow link. The former is a 155Mbps POS OC-3 link, while the latter is a 100Mbps Fast Ethernet interface. The MRTG readings are given as 6Mbps ranges, due to the limited resolution of the graphs. Note that the *pathload* estimate falls within the MRTG range in 10 out of the 12 runs, while the deviations are marginal in the two other runs.

Figure 9 shows similar results for 12 independent runs in a path between two universities in Greece. The tight (and narrow) link in this path has a capacity of 8.2Mbps. The MRTG readings are given as 1.5Mbps ranges, due to the limited resolution of the graphs. The *pathload* estimate falls

<sup>8</sup>More information about the location of the measurements hosts and the underlying routes is given in [19].



within the MRTG range in 9 out of the 12 runs, with only small errors in the three other cases.

## 6. AVAILABLE BANDWIDTH DYNAMICS

In this section, we use *pathload* to evaluate the variability of the avail-bw in different timescales and operating conditions. Given that our experiments are limited to a few paths, we do not attempt to make quantitative statements about the avail-bw variability in the Internet. Instead, our objective is to show the *relative effect* of certain operational factors on the variability of the avail-bw.

In the following experiments,  $\omega=1\text{Mbps}$  and  $\chi=1.5\text{Mbps}$ . Note that because  $\omega < \chi$ , *pathload* terminates due to the  $\omega$  constraint only if there is no grey-region; otherwise, it exits due to the  $\chi$  constraint. So, the final range  $[R^{\min}, R^{\max}]$  that *pathload* reports is either at most  $1\text{Mbps}$  ( $\omega$ ) wide, indicating that there is no grey-region, or it overestimates the width of the grey-region by at most  $2\chi$ . Thus,  $[R^{\min}, R^{\max}]$  is within  $2\chi$  (or  $\omega$ ) of the range in which the avail-bw varied during that *pathload* run. To compare the variability of the avail-bw across different operating conditions and paths, we define the following *relative variation* metric:

$$\rho = \frac{R^{\max} - R^{\min}}{(R^{\max} + R^{\min})/2} \quad (12)$$

In the following graphs, we plot the  $\{5, 15, \dots, 95\}$  percentiles of  $\rho$  based on 110 *pathload* runs for each experiment.

### 6.1 Variability and load conditions

Figure 10 shows the CDF of  $\rho$  for a path with  $C=12.4\text{Mbps}$  in three different utilization ranges of the tight link:  $u=20\text{-}30\%$ ,  $40\text{-}50\%$ , and  $75\text{-}85\%$ . Notice that *the variability of the avail-bw increases significantly as the utilization  $u$  of the tight link increases (i.e., as the avail-bw  $A$  decreases)*. This observation is not a surprise. In Markovian queues, say in  $M|M|1$ , the variance of the queueing delay is inversely proportional to the square of the avail-bw. The fact that increasing load causes higher variability was also observed for self-similar traffic in [26]. Returning to Figure 10, the 75-percentile shows that when the avail-bw is around  $A=9\text{Mbps}$  ( $u=20\text{-}30\%$ ), three quarters of the measurements have a relative variation  $\rho \leq 0.25$ . In heavy-load conditions ( $u=75\text{-}$

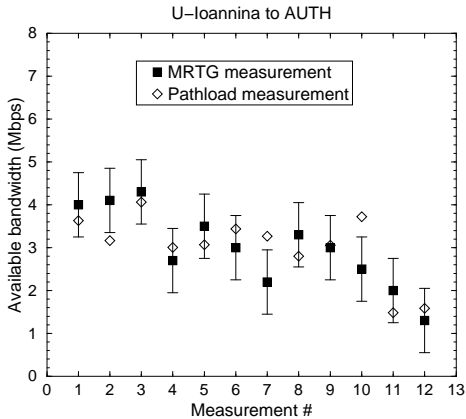


Figure 9: Verification experiment #2.

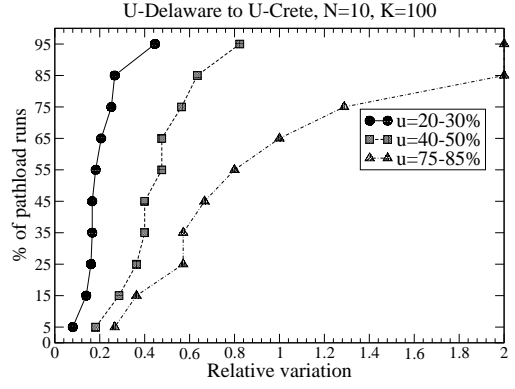


Figure 10: Variability of avail-bw in different load conditions.

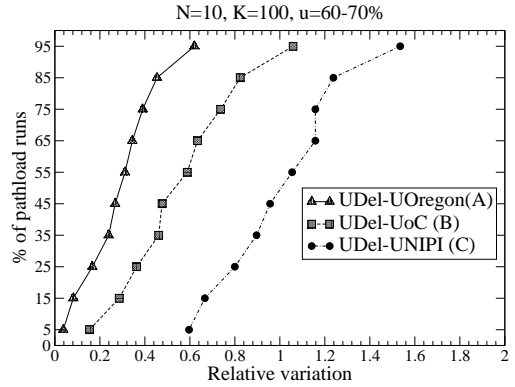


Figure 11: Variability of avail-bw in different paths.

85%) on the other hand, when  $A=2\text{-}3\text{Mbps}$ , the same fraction of measurements give almost five times higher relative variation ( $\rho \leq 1.3$ ).

We observed a similar trend in all the paths that we experimented with. For users, this suggests that a lightly loaded network will not only provide more avail-bw, but also a more predictable and smooth throughput. This latter attribute is even more important for some applications, such as streaming audio/video.

### 6.2 Variability and statistical multiplexing

In this experiment, we run *pathload* in three different paths, (A), (B), and (C), when the tight link utilization was roughly the same (around 65%) in all paths. The capacity of the tight link is  $155\text{Mbps}$  (A),  $12.4\text{Mbps}$  (B), and  $6.1\text{Mbps}$  (C). The tight link in (A) connects the Oregon GigaPoP to the Abilene network, the tight link in (B) connects a large university in Greece (Univ-Crete) to a national network (GR-net), while the tight link in (C) connects a smaller university (Univ-Pireaus) to the same national network. Based on these differences, it is reasonable to *assume* that the degree of statistical multiplexing, i.e., *the number of flows that simultaneously use the tight link*, is highest in path (A), and higher in (B) than in (C). Figure 11 shows the CDF of  $\rho$  in each path. If our assumption about the number of simultaneous flows in the tight link of these paths is correct, we observe that *the variability of the avail-bw decreases sig-*

nificantly as the degree of statistical multiplexing increases. Specifically, looking at the 75-percentile, the relative variation is  $\rho \leq 0.4$  in path (A), it increases by almost a factor of two ( $\rho \leq 0.74$ ) in path (B), and by almost a factor of three ( $\rho \leq 1.18$ ) in path (C). It should be noted, however, that there may be other differences between the three paths that cause the observed variability differences; the degree of statistical multiplexing is simply one plausible explanation.

For users, the previous measurements suggest that if they can choose between two networks that operate at about the same utilization, the network with the wider pipes, and thus with a higher degree of statistical multiplexing, will offer them a more predictable throughput. For network providers, on the other hand, it is better to aggregate traffic in a higher-capacity trunk than to split traffic in multiple parallel links of lower capacity, if they want to reduce the avail-bw variability.

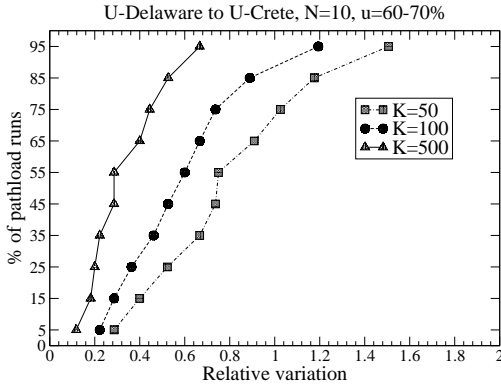


Figure 12: The effect of  $K$  on the variability of the avail-bw.

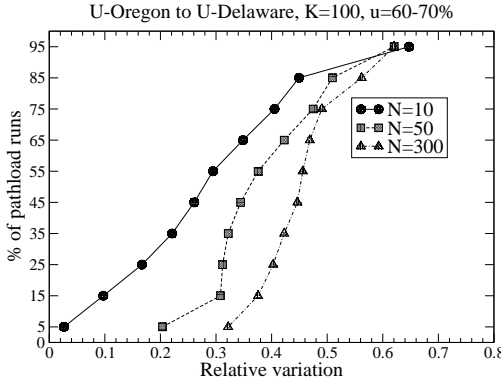


Figure 13: The effect of  $N$  on the variability of the avail-bw.

### 6.3 The effect of the stream length

Since  $V=KT$ , the stream duration  $V$  increases proportionally to the stream length  $K$ . With a longer stream, we examine whether  $R > A$  over wider timescales. As mentioned in the introduction, however, the variability of the avail-bw  $A$  decreases as the averaging timescale increases.

So, the variability in the relation between  $R$  and  $A$ , and thus the variability of the *pathload* measurements, is expected to decrease as the stream duration increases.

Figure 12 shows the CDF of  $\rho$  for three different values of  $K$  in a path with  $C=12.4$ Mbps. During the measurements,  $A$  was approximately 4.5Mbps. The stream duration  $V$  for  $R=A$ ,  $L=200$ B, and  $T=356\mu$ s is 18ms for  $K=50$ , 36ms for  $K=100$ , and 180ms for  $K=500$ . The major observation here is that the *variability of the avail-bw decreases significantly as the stream duration increases*, as expected. Specifically, when  $V=180$ ms, 75% of the measurements produced a range that is less than 2.0Mbps wide ( $\rho \leq 0.45$ ). When  $V=18$ ms, on the other hand, the corresponding maximum avail-bw range increases to 4.7Mbps ( $\rho \leq 1.05$ ).

### 6.4 The effect of the fleet length

Suppose that we measure the avail-bw  $A^\tau(t)$  in a time interval  $(t_0, t_0 + \Theta)$ , with a certain averaging timescale  $\tau$  ( $\tau < \Theta$ ). These measurements will produce a range of avail-bw values, say from a minimum  $A_{min}^\tau$  to a maximum  $A_{max}^\tau$ . If we keep  $\tau$  fixed and increase the measurement period  $\Theta$ , the range  $[A_{min}^\tau, A_{max}^\tau]$  becomes wider because it tracks the boundaries of the avail-bw process during a longer time period. An additional effect is that, as  $\Theta$  increases, the variation of the width  $A_{max}^\tau - A_{min}^\tau$  decreases. The reason is that the boundaries  $A_{min}^\tau$  and  $A_{max}^\tau$  tend to their expected values (assuming a stationary process), as the duration of the measurement increases.

The measurement period  $\Theta$  is related to the number of streams  $N$  in a fleet, and to the fleet duration  $U = N(V + \Delta)$ . As we increase  $N$ , keeping  $V$  fixed, we expand the time window in which we examine the relation between  $R$  and  $A$ , and thus we increase the likelihood that the rate  $R$  will be in the grey-region of the avail-bw ( $R \propto A$ ). So, the grey-region at the end of the *pathload* run will be wider, causing a larger relative variation  $\rho$ . This effect is shown in Figure 13 for three values of  $N$ . Observe that *as the fleet duration increases, the variability in the measured avail-bw increases*. Also, *as the fleet duration increases, the variation across different pathload runs decreases*, causing a steeper CDF.

## 7. TCP AND AVAILABLE BANDWIDTH

We next focus on the relationship between the avail-bw in a path and the throughput of a persistent (or ‘bulk’) TCP connection with arbitrarily large advertised window. There are two questions that we attempt to explore. First, can a bulk TCP connection measure the avail-bw in a path, and how *accurate* is such an avail-bw measurement approach? Second, what happens then to the rest of the traffic in the path, i.e., how *intrusive* is a TCP-based avail-bw measurement?

It is well-known that the throughput of a TCP connection can be limited by a number of factors, including the receiver’s advertised window, total transfer size, RTT, buffer size at the path routers, probability of random losses, and avail-bw in the forward and reverse paths. In the following, we use the term *Bulk Transfer Capacity (BTC) connection* (in relation to [29]) to indicate a TCP connection that is only limited by the network, and not by end-host constraints.

Let us first describe the results of an experiment that measures the throughput of a BTC connection from Univ-Ioannina (Greece) to Univ-Delaware. The TCP sender was a SunOS 5.7 box, while the TCP receiver run FreeBSD 4.3.

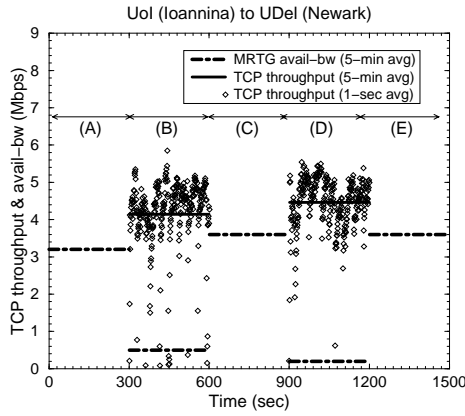


**Figure 14: Available bandwidth and BTC throughput.**

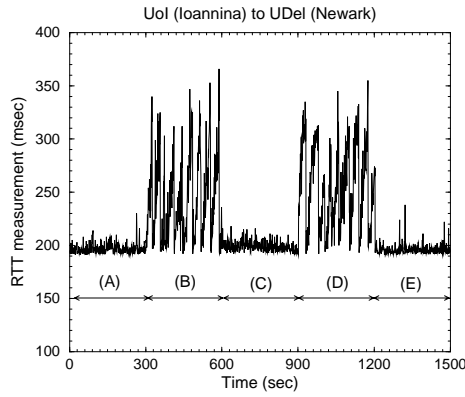


**Figure 15: RTT measurements during the experiment of Figure 14.**

The tight link in the path has a capacity of 8.2Mbps. Consider a 25-minute (min) measurement interval, partitioned in five consecutive 5-min intervals (A), (B), (C), (D), and (E). During (B) and (D) we perform a BTC connection, and measure its throughput in both 1-sec intervals and in the entire 5-min interval. During (A), (C), and (E), we do not perform a BTC connection. Throughout the 25-min interval, we also monitor the avail-bw in the path using MRTG data for each of the 5-min intervals. In parallel, we use *ping* to measure the RTT in the path at every second. Figure 14 shows the throughput of the two BTC connections, as well as the 5-min average avail-bw in the path, while Figure 15 shows the corresponding RTT measurements.

We make three important observations from these figures. First, the avail-bw during (B) and (D) is less than 0.5Mbps, and so for most practical purposes, the BTC connection manages to saturate the path. Also note, however, that the BTC throughput shows high variability when measured in 1-sec intervals, often being as low as a few hundreds of kbps. Consequently, even though a bulk TCP connection that lasts for several minutes should be able to saturate a path when not limited by the end-hosts<sup>9</sup>, shorter TCP

<sup>9</sup>This will not be the case however in under-buffered links,

connections should expect a significant variability in their throughput.

Second, there is a significant increase in the RTT measurements during (B) and (D), from a ‘quiescent point’ of 200ms to a high variability range between 200ms and 370ms. The increased RTT measurements can be explained as follows: the BTC connection increases its congestion window until a loss occurs. A loss however does not occur until the queue of the tight link overflows<sup>10</sup>. Thus, the queue size at the tight link increases significantly during the BTC connection, causing the large RTT measurements shown. To quantify the queue size increase, note that the maximum RTTs climb up to 370ms, or 170ms more than their quiescent point. The tight link has a capacity of 8.2Mbps, and so its queue size becomes occasionally at least 170KB larger during the BTC connection. The RTT jitter is also significantly higher during (B) and (D), as the queue size of the tight link varies between high and low occupancy due to the ‘sawtooth’ behavior of the BTC congestion window.

Third, the BTC connection gets an average throughput during (B) and (D), that is about 20-30% more than the avail-bw in the surrounding intervals (A), (C), and (E). This indicates that a BTC connection can get more bandwidth than what was previously available in the path, grabbing part of the throughput of other TCP connections. To see how this happens, note that the presence of the BTC connection during (B) and (D) increases the RTT of all other TCP connections that go through the tight link, because of a longer queue at that link. Additionally, the BTC connection causes buffer overflows, and thus potential losses to other TCP flows<sup>11</sup>. The increased RTTs and losses reduce the throughput of other TCP flows, allowing the BTC connection to get a larger share of the tight link than what was previously available.

To summarize, a BTC connection measures more than the avail-bw in the path, because it shares some of the previously utilized bandwidth of other TCP connections, and it causes significant increases in the delays and jitter at the tight link of its path. This latter issue is crucial for real-time and streaming applications that may be active during the BTC connection.

## 8. IS PATHLOAD INTRUSIVE?

An important question is whether *pathload* has an *intrusive behavior*, i.e., whether it causes significant decreases in the avail-bw, and increased delays or losses.

Figures 16 and 17 show the results of a 25-min experiment, performed similarly with the experiment of §7. Specifically, *pathload* runs during the 5-min intervals (B) and (D). We monitor the 5-min average avail-bw in the path using MRTG (Figure 16), and also perform RTT measurements in every 100ms (Figure 17). The RTT measurement period here is ten times smaller than in §7, because we want to examine whether *pathload* causes increased delays or losses even in smaller timescales than one second.

The results of the experiment are summarized as follows. First, the avail-bw during (B) and (D) does not show a measurable decrease compared to the intervals (A), (C), and

or paths with random losses [25].

<sup>10</sup> Assuming Drop-Tail queueing, which is the common practice today.

<sup>11</sup> We did not observe however losses of *ping* packets.

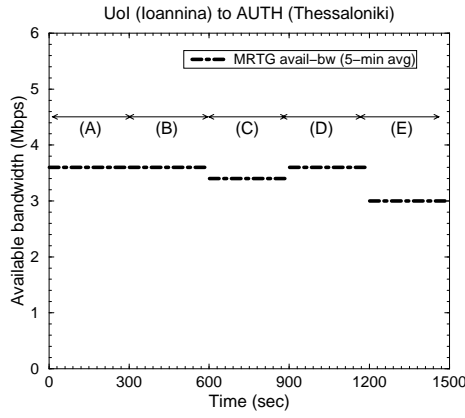


Figure 16: Available bandwidth measurements.

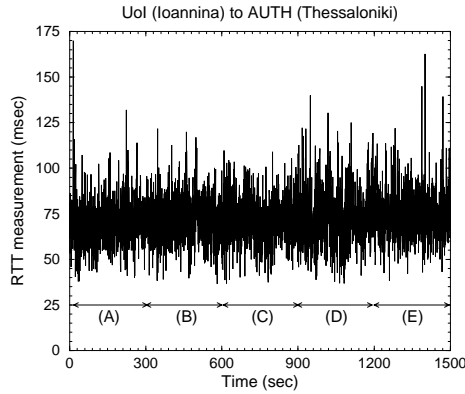


Figure 17: RTT measurements during the experiment of Figure 16.

(E). Second, the RTT measurements do not show any measurable increase when *pathload* runs. So, *pathload* does not seem to cause a persistent queue size increase, despite the fact that it often sends streams of higher rate than the avail-bw. The reason is that each stream is only  $K=100$  packets, and a stream is never sent before the previous has been acknowledged. We also note that none of the *pathload* streams encountered any losses in this experiment. None of the *ping* packets was lost either.

## 9. APPLICATIONS

An end-to-end avail-bw measurement methodology, such as SLoPS, can have numerous applications. We name a few such applications next.

**Bandwidth-Delay-Product in TCP:** Probably the most important unresolved issue in TCP is to automatically detect the *Bandwidth-Delay-Product* (BDP) of a connection. The BDP is the product of the path's avail-bw with the connection's RTT. Previous efforts attempted to get a rough estimate of the BDP using capacity, rather than avail-bw, estimation techniques [16, 2, 38]. If the avail-bw is known, it may be possible to 'jump-start' a TCP connection from that rate (with appropriate pacing though), rather than using slow-start.

**Overlay networks and end-system multicast:** The nodes of overlay networks monitor the performance of the Internet paths that interconnect them to decide how to setup overlay routes [3]. For instance, overlay networks can be used to provide end-system multicast services [11]. Existing overlays use simple RTT measurements to detect the functioning and performance of overlay network links. Equipped with real-time avail-bw measurements between nodes, overlay networks can be further optimized in terms of both routing and QoS.

**Rate adaptation in streaming applications:** Audio and video streaming applications can often adapt their transmission rate using different encoding schemes [7]. This rate adaptation process, which has been mainly driven by losses in the past, can be controlled instead by avail-bw measurements, together with congestion control constraints.

**Verification of SLAs:** Network providers often provide their customers with end-to-end (or edge-to-edge) 'virtual pipes' of a certain bandwidth [14]. It is crucial for these customers to be able to *verify*, with their own measurements, that they indeed get the bandwidth that they pay for. Measurement tools that can measure the path avail-bw, as well as capacity, in real-time and non-intrusively are of major importance for network managers.

**End-to-end admission control:** To avoid the complexities of per-flow state in network routers, [9] proposed end-point admission control. The basic idea is that the end hosts (or edge routers) probe the network by sending packets at the rate that a new flow would like to reserve. The flow is admitted if the resulting loss rate of probing packets is sufficiently low. Alternatively, the admission control test can be performed based on avail-bw measurements, avoiding the negative effect of losses.

**Server selection and anycasting:** It is often the case that clients can choose between a number of mirror servers. Clients can then use avail-bw measurements to select the best possible server. An interesting issue is to compare this technique with server selection schemes that use only RTT or short TCP transfer measurements [15].

## Acknowledgments

The authors are grateful to the following colleagues for providing us with computer accounts at their sites: C.Douligeris (Univ-Pireaus), L.Georgiadis (AUTH), E.Markatos (Univ-Crete), D.Meyer (Univ-Oregon), M.Paterakis (Technical Univ-Crete), I.Stavrakakis (Univ-Athens), and L.Tassioulas (Univ-Ioannina).

We would also like to thank the anonymous referees for their many constructive comments, as well as Melissa Seaver for her suggestions on the terminology.

## 10. REFERENCES

- [1] M. Allman. Measuring End-to-End Bulk Transfer Capacity. In *Proceedings of ACM SIGCOMM Internet Measurement Workshop*, Nov. 2001.
- [2] M. Allman and V. Paxson. On Estimating End-to-End Network Path Properties. In *Proceedings of ACM SIGCOMM*, Sept. 1999.
- [3] D. Andersen, H. Balakrishnan, F. Kaashoek, and R. Morris. Resilient Overlay Networks. In *Proceedings of ACM Symposium on Operating Systems Principles*, Oct. 2001.

- [4] A. A. Awadallah and C. Rai. TCP-BFA: Buffer Fill Avoidance. In *Proceedings of IFIP High Performance Networking Conference*, Sept. 1998.
- [5] H. Balakrishnan, S. Seshan, M. Stemm, and R. H. Katz. Analyzing Stability in Wide-Area Network Performance. In *Proceedings of ACM SIGMETRICS*, June 1997.
- [6] S. Banerjee and A. K. Agrawala. Estimating Available Capacity of a Network Connection. In *Proceedings IEEE International Conference on Networks*, Sept. 2001.
- [7] J. C. Bolot and T. Turletti. A Rate Control Mechanism for Packet Video in the Internet. In *Proceedings of IEEE INFOCOM*, pages 1216–1223, June 1994.
- [8] L. S. Brakmo, S. W. O'Malley, and L. L. Peterson. TCP Vegas: New Techniques for Congestion Detection and Avoidance. In *Proceedings of ACM SIGCOMM*, Aug. 1994.
- [9] L. Breslau, E. Knightly, S. Shenker, I. Stoica, and H. Zhang. Endpoint Admission Control: Architectural Issues and Performance. In *Proceedings of ACM SIGCOMM*, 2000.
- [10] R. L. Carter and M. E. Crovella. Measuring Bottleneck Link Speed in Packet-Switched Networks. *Performance Evaluation*, 27,28:297–318, 1996.
- [11] Y.-H. Chu, S. G. Rao, S. Seshan, and H. Zhang. Enabling Conferencing Applications on the Internet using an Overlay Multicast Architecture. In *Proceedings of ACM SIGCOMM*, Aug. 2001.
- [12] C. Dovrolis, P. Ramanathan, and D. Moore. What do Packet Dispersion Techniques Measure? In *Proceedings of IEEE INFOCOM*, pages 905–914, Apr. 2001.
- [13] A. Downey. Using Pathchar to Estimate Internet Link Characteristics. In *Proceedings of ACM SIGCOMM*, Sept. 1999.
- [14] N. Duffield, P. Goyal, A. Greenberg, P. Mishra, K. K. Ramakrishnan, and J. E. Merwe. A Flexible Model for Resource Management in Virtual Private Networks. In *Proceedings of ACM SIGCOMM*, Sept. 1999.
- [15] K. M. Hanna, N. Natarajan, and B. N. Levine. Evaluation of a Novel Two-Step Server Selection Metric. In *Proceedings International Conference on Network Protocols (ICNP)*, Oct. 2001.
- [16] J. Hoe. Improving the Start-up Behavior of a Congestion Control Scheme for TCP. In *Proceedings of ACM SIGCOMM*, Sept. 1996.
- [17] V. Jacobson. Congestion Avoidance and Control. In *Proceedings of ACM SIGCOMM*, pages 314–329, Sept. 1988.
- [18] V. Jacobson. Pathchar: A Tool to Infer Characteristics of Internet Paths. <ftp://ftp.ee.lbl.gov/pathchar/>, Apr. 1997.
- [19] M. Jain and C. Dovrolis. Pathload: A measurement tool for end-to-end available bandwidth. In *Proceedings of Passive and Active Measurements (PAM) Workshop*, Mar. 2002.
- [20] R. Jain. A delay-based approach for congestion avoidance in interconnected heterogeneous computer networks. *ACM Computer Communications Review*, 19(5):56–71, Oct. 1989.
- [21] G. Jin, G. Yang, B. Crowley, and D. Agarwal. Network Characterization Service (NCS). In *Proceedings of 10th IEEE Symposium on High Performance Distributed Computing*, Aug. 2001.
- [22] S. Keshav. A Control-Theoretic Approach to Flow Control. In *Proceedings of ACM SIGCOMM*, Sept. 1991.
- [23] K. Lai and M. Baker. Measuring Bandwidth. In *Proceedings of IEEE INFOCOM*, Apr. 1999.
- [24] K. Lai and M. Baker. Measuring Link Bandwidths Using a Deterministic Model of Packet Delay. In *Proceedings of ACM SIGCOMM*, Sept. 2000.
- [25] T. V. Lakshman and U. Madhow. The performance of TCP/IP for networks with high bandwidth-delay products and random losses. *IEEE/ACM Transactions on Networking*, 5(3):336–350, June 1997.
- [26] W. E. Leland, M. S. Taqqu, W. Willinger, and D. V. Wilson. On the Self-Similar Nature of Ethernet Traffic (Extended Version). *IEEE/ACM Transactions on Networking*, 2(1):1–15, Feb. 1994.
- [27] B. A. Mah. pchar: a Tool for Measuring Internet Path Characteristics. <http://www.employees.org/~bmah/Software/pchar/>, Feb. 1999.
- [28] M. Mathis. *TReno Bulk Transfer Capacity*, Feb. 1999. IETF Internet Draft draft-ietf-ippm-reno-btc-03.txt (work-in-progress).
- [29] M. Mathis and M. Allman. *A Framework for Defining Empirical Bulk Transfer Capacity Metrics*, July 2001. RFC 3148.
- [30] B. Melander, M. Bjorkman, and P. Gunningberg. A New End-to-End Probing and Analysis Method for Estimating Bandwidth Bottlenecks. In *Global Internet Symposium*, 2000.
- [31] D. Mitra and J. B. Seery. Dynamic adaptive windows for high-speed data networks: theory and simulations. In *Proceedings of ACM SIGCOMM*, Aug. 1990.
- [32] NSv2. Network Simulator. <http://www.isi.edu/nsnam/ns/>.
- [33] T. Oetiker. MRTG: Multi Router Traffic Grapher. <http://ee-staff.ethz.ch/~oetiker/webtools/mrtg/mrtg.html>.
- [34] A. Pasztor and D. Veitch. The Packet Size Dependence of Packet Pair Like Methods. In *IEEE/IFIP International Workshop on Quality of Service (IWQoS)*, 2002.
- [35] V. Paxson. On Calibrating Measurements of Packet Transit Times. In *Proceedings of ACM SIGMETRICS*, June 1998.
- [36] V. Paxson. End-to-End Internet Packet Dynamics. *IEEE/ACM Transaction on Networking*, 7(3):277–292, June 1999.
- [37] V. Ribeiro, M. Coates, R. Riedi, S. Sarvotham, B. Hendricks, and R. Baraniuk. Multifractal Cross-Traffic Estimation. In *Proceedings ITC Specialist Seminar on IP Traffic Measurement, Modeling, and Management*, Sept. 2000.

- [38] Web100. Automatic Bandwidth Delay Product Discovery.  
http://www.web100.org/docs/archive/bdp.discovery.php, 2001.
- [39] Y. Zhang, N. Duffield, V. Paxson, and S. Shenker. On the Constancy of Internet Path Properties. In *Proceedings of ACM SIGCOMM Internet Measurement Workshop*, Nov. 2001.

## APPENDIX

### A. PROOF OF PROPOSITION 1

#### A.1 At the first link

Case 1:  $R_0 > A_1$ .

Suppose that  $t^k$  is the arrival time of packet  $k$  in the queue. Over the interval  $[t^k, t^k + T)$ , with  $T = L/R_0$ , the link is constantly backlogged because the arriving rate is higher than the capacity ( $R_0 + u_1 C_1 = C_1 + (R_0 - A_1) > C_1$ ). Over the same interval, the link receives  $L + u_1 C_1 T$  bytes and services  $C_1 T$  bytes. Thus,

$$\Delta q_1^k = (L + u_1 C_1 T) - C_1 T = (R_0 - A_1) T > 0 \quad (13)$$

and so,

$$\Delta d_1^k = \frac{R_0 - A_1}{C_1} T > 0. \quad (14)$$

Packet  $k+1$  departs the first link  $\Lambda$  time units after packet  $k$ , where

$$\Lambda = (t^{k+1} + d_1^{k+1}) - (t^k + d_1^k) = T + \frac{R_0 - A_1}{C_1} T \quad (15)$$

that is independent of  $k$ . So, *the packets of the stream depart the first link with a constant rate  $R_1$* , where

$$R_1 = \frac{L}{\Lambda} = R_0 \frac{C_1}{C_1 + (R_0 - A_1)}. \quad (16)$$

We refer to rate  $R_{i-1}$  as the *entry-rate* in link  $i$ , and to  $R_i$  as the *exit-rate* from link  $i$ . Given that  $R_0 > A_1$  and that  $C_1 \geq A_1$ , it is easy to show that *the exit-rate from link 1 is larger or equal than  $A_1$ <sup>12</sup> and lower than the entry-rate*,

$$A_1 \leq R_1 < R_0. \quad (17)$$

Case 2:  $R_0 \leq A_1$ .

In this case, the arrival rate at the link in interval  $[t^k, t^k + T)$  is  $R_0 + u_1 C_1 \leq C_1$ . So, packet  $k$  is serviced before packet  $k+1$  arrives at the queue. Thus,

$$\Delta q_1^k = 0, \quad \Delta d_1^k = 0, \quad \text{and} \quad R_1 = R_0 \quad (18)$$

#### A.2 Induction to subsequent links

The results that were previously derived for the first link can be proved inductively for each link in the path. So, we have the following relationship between the entry and exit rates of link  $i$ :

$$R_i = \begin{cases} R_{i-1} \frac{C_i}{C_i + (R_{i-1} - A_i)} & \text{if } R_{i-1} > A_i \\ R_{i-1} & \text{otherwise} \end{cases} \quad (19)$$

with

$$A_i \leq R_i < R_{i-1} \quad \text{when } R_{i-1} > A_i \quad (20)$$

<sup>12</sup>  $R_1 = A_1$  when  $A_1 = C_1$ .

Consequently, the exit-rate from link  $i$  is

$$R_i \geq \min\{R_{i-1}, A_i\} \quad (21)$$

Also, the queueing delay difference between successive packets at link  $i$  is

$$\Delta d_i^k = \begin{cases} \frac{R_{i-1} - A_i}{C_i} T > 0 & \text{if } R_{i-1} > A_i \\ 0 & \text{otherwise} \end{cases} \quad (22)$$

### A.3 OWD variations

If  $R_0 > A$ , we can apply (20) recursively for  $i = 1, \dots, (t-1)$  to show that the stream will arrive at the tight link with a rate  $R_{t-1} \geq A_{t-1} > A_t$ . Thus, based on (22),  $\Delta d_t^k > 0$ , and so the OWD difference between successive packets will be positive,  $\Delta d^k > 0$ .

On the other hand, if  $R_0 \leq A$ , then  $R_0 \leq A_i$  for every link  $i$  (from the definition of  $A$ ). So, applying (21) recursively from the first link to the last, we see that  $R_i < A_i$  for  $i = 1, \dots, H$ . Thus, (22) shows that the delay difference in each link  $i$  is  $\Delta d_i^k = 0$ , and so the OWD differences are  $\Delta d^k = 0$ .

## B. VERIFICATION USING MRTG

MRTG is a widely used tool that displays the utilized bandwidth of a link, based on information that comes directly from the router interface [33]. Specifically, MRTG periodically reads the number of bytes sent and received from the router's Management Information Base using the SNMP protocol. The default measurement period is 5 minutes, and thus the MRTG bandwidth readings should be interpreted as 5-min averages. If the capacity of the link is also known, the avail-bw in the same time interval is the capacity minus the utilized bandwidth (see Equation 2). Figure 18 shows

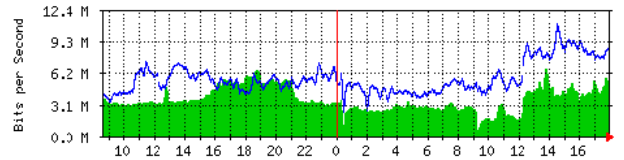


**Figure 18: Example of an MRTG graph for a 12.4Mbps link. The x-axis is measured in hours.**

a snapshot of an MRTG graph for a 12.4Mbps duplex link. The two curves (shaded vs line) refer to the two directions of the link (IN vs OUT).

MRTG offers a crude way to verify *pathload*, giving us 5-min averages for the avail-bw of individual links in the path. In the paths that we experimented with, we have access to MRTG graphs for mosts links in the path (especially for the most heavily utilized links), as well as information about their capacity. The tight link remains the same for the duration of many hours in these paths, and so the measurement of end-to-end avail-bw is based on a single MRTG graph, that of the tight link.